Departures from local thermodynamic equilibrium in cutting arc plasmas derived from electron and gas density measurements using a two-wavelength quantitative Schlieren technique

L. Prevosto,[1,a)] G. Artana,[2] H. Kelly,[1,3] and B. Mancinelli[1]
[1]*Grupo de Descargas Eléctricas, Departamento Ing. Electromecánica, Facultad Regional Venado Tuerto (UTN), Laprida 651, Venado Tuerto 2600, Santa Fe, Argentina*
[2]*Laboratorio de Fluidodinámica, Departamento Ing. Mecánica, Facultad de Ingeniería (UBA), Paseo Colon 850, C1063ACV, Buenos Aires, Argentina*
[3]*Departamento de Física, Facultad de Ciencias Exactas y Naturales (UBA), Instituto de Física del Plasma (CONICET), Ciudad Universitaria, Pab. I, 1428 Buenos Aires, Argentina*

(Received 6 September 2010; accepted 23 December 2010; published online 16 March 2011)

A two-wavelength quantitative Schlieren technique that allows inferring the electron and gas densities of axisymmetric arc plasmas without imposing any assumption regarding statistical equilibrium models is reported. This technique was applied to the study of local thermodynamic equilibrium (LTE) departures within the core of a 30 A high-energy density cutting arc. In order to derive the electron and heavy particle temperatures from the inferred density profiles, a generalized two-temperature Saha equation together with the plasma equation of state and the quasineutrality condition were employed. Factors such as arc fluctuations that influence the accuracy of the measurements and the validity of the assumptions used to derive the plasma species temperature were considered. Significant deviations from chemical equilibrium as well as kinetic equilibrium were found at elevated electron temperatures and gas densities toward the arc core edge. An electron temperature profile nearly constant through the arc core with a value of about 14 000–15 000 K, well decoupled from the heavy particle temperature of about 1500 K at the arc core edge, was inferred. © *2011 American Institute of Physics*. [doi:10.1063/1.3552304]

I. INTRODUCTION

Very high heat fluxes (up to 10^{10} W m^{-2} in the jet core), extremely high plasma enthalpies ($\approx 10^8$ J kg^{-1}), and high plasma velocities (M > 1, M being the Mach number), are a few of the primary features of cutting arc plasmas.[1] Such arcs are created by a narrow nozzle ($\approx$1 mm) inside a torch, where a gas is tangentially injected at high pressure. The intense gas-vortex convective cooling at the arc fringes enhances power dissipation in the arc column ($\approx 10^{12}$ W m^{-3}) resulting in extremely sharp plasma quantity gradients and very high electric field strengths ($\approx 10^4$ V m^{-1}), which, in turn, may produce significant deviations from local thermodynamic equilibrium (LTE).[2,3]

In general, disturbances of an LTE situation in arc plasmas may occur in three different ways:[2] (1) deviation from excitation equilibrium, i.e., the population of the excited states does not follow a Boltzmann distribution; (2) deviation from chemical equilibrium, i.e., the electron and gas densities cannot be described by the classical Saha equation in terms of a single species temperature; and (3) deviation from kinetic equilibrium, i.e., the electron and heavy particle temperature are not the same. For case (1), the term partial local thermodynamic equilibrium (PLTE) has been introduced, in contrast to a complete local thermodynamic equilibrium situation, for which none of the above-mentioned deviations occurs. As soon as the electron density in the plasma drops below a certain critical value, deviations from the chemical equilibrium [case (2)] will occur, and the classical Saha equation no longer provides an adequate description of the actual plasma composition. On the other hand, in regions where sharp but nonuniform plasma quantity gradients exist, as in case (3), deviations from the chemical equilibrium will occur by convective and diffusive particle fluxes that can cause differences in the actual rate constants from their chemical equilibrium values.

According to Griem's criterion,[2] LTE exists inside an optical thin plasma volume only when the electron density exceeds $\approx 10^{23}$ m^{-3}. LTE further requires that local gradients of the plasma quantities be sufficiently small (i.e., the diffusion time should be of the same order of magnitude or larger than the equipartition energy time) and that the local electric field strength also be small.[2] As a consequence, LTE might hold only inside the core of high-current arcs at atmospheric pressure or above. However, numerous analytical models as well as experimental studies have demonstrated that departures from LTE are very common in high-pressure arcs.

For free burning argon arcs, nonequilibrium plasma models have shown significant discrepancies from LTE at elevated electron temperatures at the arc fringes,[4] as well as near the electrodes.[5–7] By using line shape analysis of scattered laser light, electron temperatures higher than heavy particle temperatures by as much as 7000 K were inferred for an electron density of 1.6×10^{23} m^{-3} in a free burning argon arc.[8] A similar deviation from LTE (electron temperature at least 4000 K higher than the gas temperature) was then confirmed by other researchers also using scattering

a)Electronic mail: prevosto@waycom.com.ar.

measurements in the same kind of arcs.[9] These studies focused on thick (weldinglike) arcs.

Most of the developed numerical models for cutting arcs were based on LTE.[10–14] Recently, a two-temperature, chemical nonequilibrium model inside the nozzle of a 200 A oxygen cutting arc has been reported.[15] Calculated values of electron temperature were at all locations higher than the heavy particle temperature values, with a difference of up to 3000 K on the axis and of ≈11 000 K near the nozzle wall. More recently, departures from LTE were experimentally reported inside the nozzle of a 30 A high-energy density cutting torch by analyzing the nozzle current–voltage characteristic curve.[16,17] An electron temperature of about 5000 K was inferred near the wall, well decoupled from the heavy particle temperature (of about 1000 K).

Experimental data on cutting arcs are somewhat scarce and are mostly related to spectroscopic measurements in the external plasma region.[1] In emission spectroscopic investigations the LTE assumption is often used to derive the temperature from the excited emitting particle population. This assumption implies that collisions are the dominant mechanism governing each species population, and that the temperature and concentration gradients are low, which is not the case at the arc fringes or close to electrodes or solid walls. The electron density can be measured from the line profiles, which depend mainly on the Stark broadening effect in high pressure plasmas.[2,3] In determining the density of the other species, the problem is more complex and assumptions are mandatory.[2,3,18] In practice, all of the available spectroscopic data for cutting arcs are used to derive electron concentrations and single plasma temperatures (using the LTE assumption).[11,12,19–21]

A quantitative Schlieren investigation[22] with cutting arcs using a single continuous laser (wavelength of 632.8 nm) as the light source has been reported in previous work by the authors.[23] This diagnostic determined the electron density radial profile. The purpose of the current work is to present an extension of that work using two different lasers (wavelengths of 632.8 and 514 nm) that will allow inference of the electron as well as the gas densities without imposing any assumption regarding statistical equilibrium models. As an example, the developed technique was used for the study of LTE departures in a 30 A high-energy density cutting arc at 3.5 mm from the nozzle exit. In order to derive the electron and heavy particle temperatures from the inferred density profiles, a generalized two-temperature Saha equation[24] (instead of the classical Saha equation) together with the plasma equation of state and the quasineutrality condition were employed. It is assumed in this investigation that possible deviations from chemical equilibrium due to convective and diffusive particle fluxes are negligible.

In the Sec. II the experimental arrangement is presented. The obtained experimental data and its interpretation are given in Sec. III. The conclusions are summarized in Sec. IV.

II. EXPERIMENTAL ARRANGEMENT

The high-energy density cutting torch used in this study consisted of a copper cathode (7 mm in diameter) centered above an orifice in a nozzle with liquid cooling (Fig. 1). A flow of oxygen gas cooled the cathode and was also employed as the plasma gas. The gas passed through a swirl ring to provide arc stability. The nozzle had a converging-straight bore (with a bore radius of 0.5 mm and a length of 4.5 mm) in a copper holder surrounding the cathode. To avoid plasma contamination by metal vapors from the anode, a rotating steel disk (rotating frequency of 23 s^{-1}), 200 mm in diameter and 11 mm thick, was used as the anode.[3,5] The disk upper surface was located 8 mm from the nozzle exit. A well-stabilized arc column was obtained, and the lateral surface of the anode disk was completely unmelted. Thus, almost no metal vapors from the anode were present in the arc. During the experiment the arc current and the gas mass flow rate were kept constant at 30 A and 0.71 g s^{-1}, respectively. The DC level of the arc voltage was ≈180 V with a superimposed oscillatory component with a frequency of 150 Hz (due to the ripple of the arc power source) that amounts to <3% of the DC component. More details on the torch characteristics can be found elsewhere.[25]

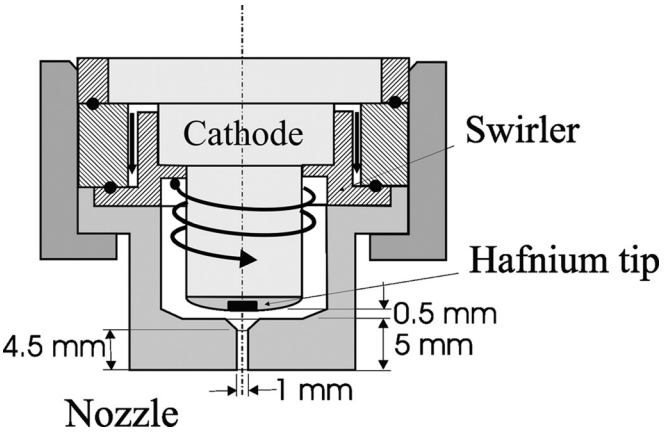

FIG. 1. Schematic of the arc torch indicating several geometric dimensions.

A Z-type two-mirror Schlieren system was used in this research.[22] The system included two 20 mW continuous lasers with main wavelengths of 632.8 and 514 nm as the light sources. Figure 2 shows a schematic of the experimental setup. The laser beams were focused onto the center of a (50/50) beam splitter, one of them (514 nm) impinging on the splitter front face with the other (632.8 nm) impinging on the splitter back face. The two beams were aligned on the optical axis of the system by using two mirrors (M_1 and M_2, see Fig. 2) that could be accurately controlled by 2D micrometers. The laser beams were then expanded to a diameter of ≈100 mm at the first parabolic mirror surface (M_3 in Fig. 2, with 100 mm diameter and a focal distance $f_1 = 900$ mm) by using an optical expansion system. This mirror serves to collimate the incoming beams. A second parabolic mirror (M_4 in Fig. 2, with 100 mm diameter and a focal distance $f_2 = 1100$ mm) formed an image of the observation region (nozzle exit, cutting arc, and lateral surface of the anode in this case) on a white screen. A knife-edge with $x-z$ movements (see coordinates indicated in Fig. 2) that could be accurately controlled by a 2D micrometer was located between M_4 and the screen, at the focus of the mirror.

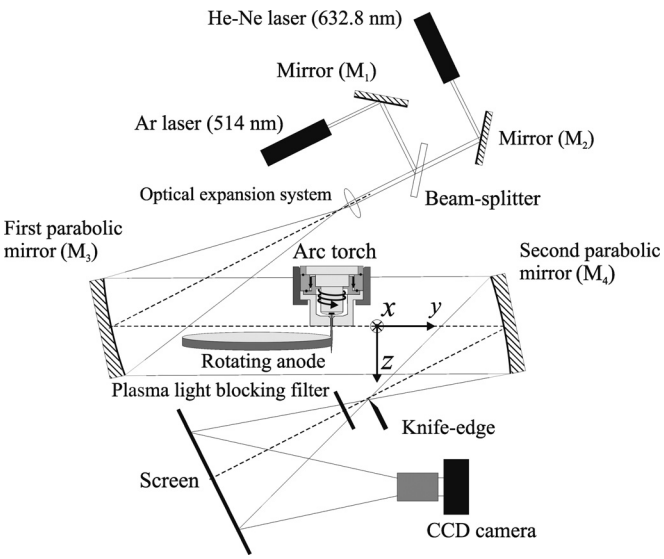

FIG. 2. Schematic of the Z-type two-wavelength Schlieren system.

The cutting torch was positioned vertically with the streamwise direction of the plasma flow along the z direction ($z=0$ corresponds to the nozzle exit), and the knife-edge was positioned parallel to this direction to provide the best sensibility perpendicular to the arc axis. Two bandpass filters centered at each laser wavelength were alternatively used to block the plasma light emitted from the arc. Simply by turning (on/off) one laser while the other is the opposite, several independent Schlieren images of the arc for each light wavelength were obtained within a single arc run. The Schlieren images (with a size of 768×484 pixels) were acquired with a PULNiX TM-9701 CCD digital camera at an exposure time of 1/250 s. These images were stored in PNG format and digitized by an 8-bit gray-scale frame grabber. According to the magnification of this optical system, the spatial resolution in the Schlieren image was about 0.05 mm (20 pixels corresponds to 1 mm).

III. EXPERIMENTAL RESULTS AND DISCUSSION

The plasma refractivity [$(n-1)$, n being the refraction index of the medium] for a laser light of wavelength (λ), is given by[23]

$$n - 1 = -\frac{N_e e^2 \lambda^2}{8\pi^2 c^2 \varepsilon_0 m_e} + \frac{1}{4\pi\varepsilon_0} 2\alpha_n N_n, \qquad (1)$$

where N_e is the electron density, e is the electronic charge, m_e is the electron mass, ε_0 is the free space permittivity, c is the speed of light, α_n is the polarizability of neutrals (only slightly dependent on the light wavelength),[22] and N_n, the neutral density. The first term on the right-hand side of Eq. (1) is the electron contribution (strongly dependent on the light wavelength), while the second is the neutral (gas) contribution. For the experimental conditions considered here, Eq. (1) is valid for optical (or shorter) wavelengths.[23]

It is well known that when a light ray passes through an inhomogeneous medium, it suffers a deviation in its trajectory by a certain angle that depends both, on the refractive index and on the thickness of the medium under test. Such ray path deviations can alter the local illuminance on the screen only if the deviations are weak enough (i.e., when the measuring range of the Schlieren system has not been exceeded).[22] When this condition is satisfied, the contrast C of the light pattern on the screen (defined as the ratio of the differential illuminance at a given image pixel to the value of its background level illuminance) is the output of the Schlieren system.[22] By assuming circular symmetry in the arc,[23] the contrast is given by

$$C(x,z) \approx 2\frac{f_2}{a\, n_\infty}\int_0^\infty \frac{\partial n}{\partial r}\frac{x}{r}dy, \qquad (2)$$

where n_∞ is the refraction index of the surrounding medium, a represents the height of the image (measured from the knife-edge, and without the presence of the tested medium) and r is the radial coordinate measured from the arc axis. More details on the development of this quantitative Schlieren technique can be found in a previous work.[23]

Using the experimental C data and the Abel inversion technique,[18,23] Eq. (2) can be inverted to obtain the radial profile (for a given z value) of the plasma refraction index for $\lambda = 514$ and 632.8 nm. Then, using Eq. (1), a straightforward calculation for the electron and gas densities is given by

$$N_e \approx \left(8\pi^2 c^2 \varepsilon_0 m_e / e^2\right)\frac{n_g - n_r}{\lambda_r^2 - \lambda_g^2}, \qquad (3)$$

$$N_n \approx \left[n_g\left(1+\frac{\lambda_r^2+\lambda_g^2}{\lambda_r^2-\lambda_g^2}\right) + n_r\left(1-\frac{\lambda_r^2+\lambda_g^2}{\lambda_r^2-\lambda_g^2}\right) - 2\right]\frac{\pi\varepsilon_0}{\alpha_n}, \qquad (4)$$

where the subscripts (r) and (g) indicate quantities related to the wavelengths 632.8 and 514 nm, respectively. Note that Eqs. (3) and (4) allow obtaining the electron and gas densities.

Several arc Schlieren images for $\lambda = 514$ and 632.8 nm were obtained in a single arc run. A typical 30 A arc Schlieren image for $\lambda = 514$ nm is shown in Fig. 3. In this case, the knife-edge was located so as to cut ≈50% of the unperturbed perpendicular beam. Since the knife-edge was placed vertically (cutting on the left side of the image), positive plasma density radial gradients (directed to the right side of the image) are visualized as light areas, and negative gradients as dark ones.[22]

Note that a horizontal straight line corresponding to $z = 3.5$ mm has been inserted in Fig. 3, corresponding to the arc axial position that was chosen for performance of the radial inversion. The 3.5 mm position was chosen for two reasons: first, because this arc section was previously studied in several works,[23,25] thus allowing a direct comparison with the present results; second, to derive the electron and heavy particle temperatures, it is necessary to use a generalized two-temperature Saha equation[24] and the state equations, which in turn require knowledge of the arc pressure. It is a well-known fact that in this kind of arc there is an underexpanded jet at the nozzle exit, and the arc reaches

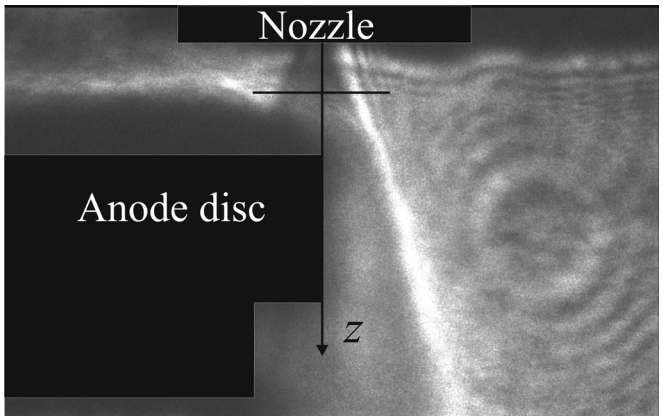

FIG. 3. Typical gray-scale Schlieren image of the 30 A high-energy density cutting arc for $\lambda = 514$ nm. The percentage of the knife-edge cutoff was $\approx 50\%$ (blocking on the left side of the laser beam). The straight horizontal line indicates the section $z = 3.5$ mm.

atmospheric pressure downstream through a shock front that appears about 1–2 mm from the nozzle exit.[11,12] Hence, at $z = 3.5$ mm arc pressure can be considered constant in the radial direction and equal to the atmospheric value.

An important point to discuss is that the radial interval (if any) within the inversion can be taken with confidence. In Fig. 4(a) an ion current waveform obtained at $z = 3.5$ mm from a sweeping probe[25] is presented. The horizontal temporal scale can be easily transformed in a spatial scale taking into account the probe sweeping velocity (18 m s^{-1} in this case). This signal is proportional to the plasma density.[25] It can be seen from Fig. 4(a) that the current signal has an approximately rectangular shape, with a spatial width of about 0.6 mm (corresponding to an arc radius of about 0.3 mm). This shape was quite reproducible with statistical fluctuations smaller than 3%. Since the technique developed in this work is based on the difference between refraction indexes at two different wavelengths, and since the electron contribution is the only part strongly dependent on λ, it is clear that the technique will be sensitive only within arc regions where the electron density is high. So in this case $r < 0.3$ mm was taken as an upper limit for the Schlieren inversion.

In Fig. 4(b) the mean values of the refraction indexes corresponding to the two λ values and for $z = 3.5$ mm are presented including the corresponding error bars. Since the Schlieren images were taken at different times (but within a single arc run) the inversion procedure is affected mainly by statistical uncertainties due to arc fluctuations associated with voltage variations from the power source (i.e., voltage ripple). There is an additional source of error related to uncertainty in the a value ($\approx 2.5\%$). In practice, the uncertainties in Fig. 4(b) represent both these sources, where the statistical one was taken into account by considering the standard error of the mean of five different Schlieren images taken within a single arc run. Note in Fig. 4(b) that in the arc central region ($r < 0.3$ mm) both refraction indexes are well separated (as a consequence of a good statistical reproducibility) beyond the error bands (in this region the standard error of the mean refractivities is about 5%), but at the arc periphery there is strong overlapping between them, within large statistical band errors (standard error of the mean refractivities is about 25%). As a review, Figures 4(a) and 4(b) indicate that the results of the developed technique can be taken with confidence for $r < 0.3$ mm, with a space resolution of 0.05 mm.

Using Eqs. (3) and (4), the calculated electron and gas densities (with their corresponding uncertainty ranges) derived from the refraction index profiles shown in Fig. 4(b), are given in Fig. 5. Typically, the uncertainty in N_e values is around 30% (derived from the uncertainties in the refractive indexes) while that of the N_n values is around 60%. For comparative purposes, the corresponding density values previously obtained by the authors using a single wavelength Schlieren technique together with the LTE assumption[23] are

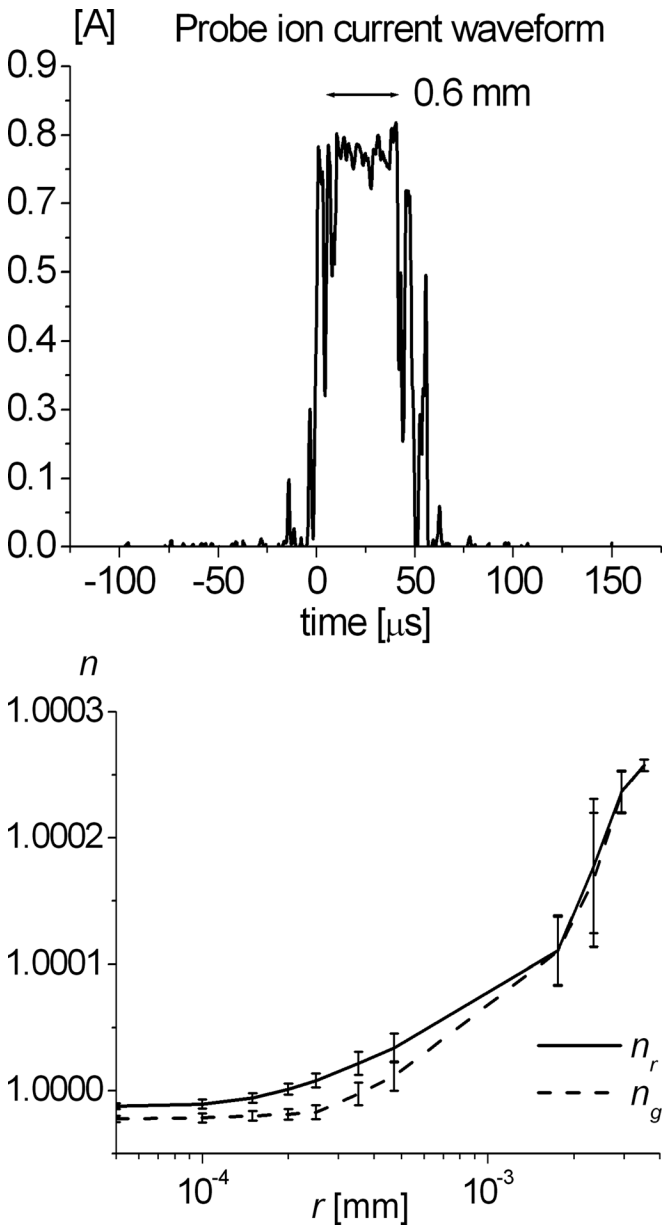

FIG. 4. (a) Ion current waveform obtained from a sweeping probe at z = 3.5 mm. The probe sweeping velocity was 18 m s^{-1}. (b) Calculated radial profiles of the arc refraction indexes (with their corresponding uncertainty ranges) at $z = 3.5$ mm for $\lambda = 632.8$ and 514 nm.

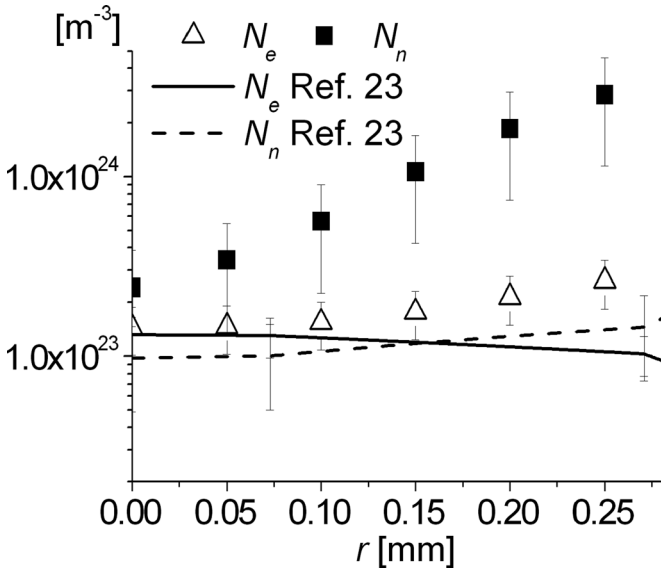

FIG. 5. Calculated electron and gas density profiles (with their corresponding uncertainty ranges) derived from the refraction index profiles shown in Fig. 4(b). For comparative purposes, the corresponding density values previously obtained by the authors (Ref. 23) are also shown. Reprinted with permission from L. Prevosto, G. Artana, B. Mancinelli, and H. Kelly, J. Appl. Phys. **107**, 023304 (2010). Copyright © 2010 American Institute of Physics.

also shown in Fig. 5. As can be seen, no significant differences appear between the electron density profiles along the arc core. On the hand, marked differences (larger than 100%) between the obtained gas density values and those found in earlier work[23] (for $T = T_h = T_e$, T_e and T_h being the electron and heavy particle temperature, respectively), appear toward the arc core edge.

As state in Sec. I, to derive the electron and heavy particle temperatures from the inferred density profiles a generalized two-temperature Saha equation, together with the equation of state (for a plasma pressure of one atmosphere); were used. A generalized Saha equation can be used because significant deviations from chemical equilibrium due to convective/diffusive particle fluxes are not expected (these deviations are solely expected in regions where a marked widening or a marked constriction of the arc occurs;[15,26] not at the studied arc region where the arc exhibits a well-defined cylindrical shape[27]). These equations are as follows[24]

$$\frac{N_e\, N_i}{N_n} = 2\frac{Q_i}{Q_0}\left(\frac{2\,\pi\, m_e\, k\, T_e}{h^2}\right)^{3/2} \exp\left(-\frac{E_I}{k\, T_e}\right), \qquad (5)$$

$$p = k\,[N_e\, T_e + (N_i + N_n)\, T_h], \qquad (6)$$

where N_i is the ion density, Q_i and Q_o are the statistical weights of oxygen ions and atoms respectively, k is Boltzmann's constant, h is the Planck constant, and E_I is the ionization energy of the oxygen atom. Also, the neutrality equation for the plasma was used

$$N_i \cong N_e. \qquad (7)$$

Equations (5)–(7) form a closed set for the unknowns T_e, T_h, and N_i for given values of N_e and N_n.

In Fig. 6 the electron and heavy particle temperatures derived from the density values of Fig. 5 are presented. In this case the typical uncertainties are around 15% for T_e and 30% for T_h. For comparative purposes, the equilibrium LTE plasma temperature (T) previously derived[23] is also shown in Fig. 6. A strong increase in the difference between both temperature profiles is observed along the arc core; reaching about 11 000 K at the arc core edge ($r \approx 0.25$ mm). The magnitude of this difference is comparable to or larger than those reported by using a nonequilibrium model for a 200 A oxygen cutting torch.[15] It is also shown that the electron temperature as well as the LTE temperature[23] remains nearly constant through the arc core, with similar values of about 14 000–15 000 K.

IV. CONCLUSIONS

A two-wavelength quantitative Schlieren technique that allows inferring the electron as well as the gas densities of axisymmetric plasmas without imposing any assumption regarding statistical equilibrium models has been developed.

The technique was applied to the study of LTE departures in the core of a 30 A high-energy density cutting arc at 3.5 mm from the nozzle exit. That distance was chosen because at this location the arc pressure becomes the atmospheric value, and also because several previous studies were performed at this location, allowing a comparison of results. In order to derive the electron and heavy particle temperatures from the inferred density profiles, a generalized two-temperature Saha equation together with the plasma equation of state and the quasineutrality condition were employed. Statistical arc fluctuations that influence the accuracy of the measurements were considered. This study has shown that:

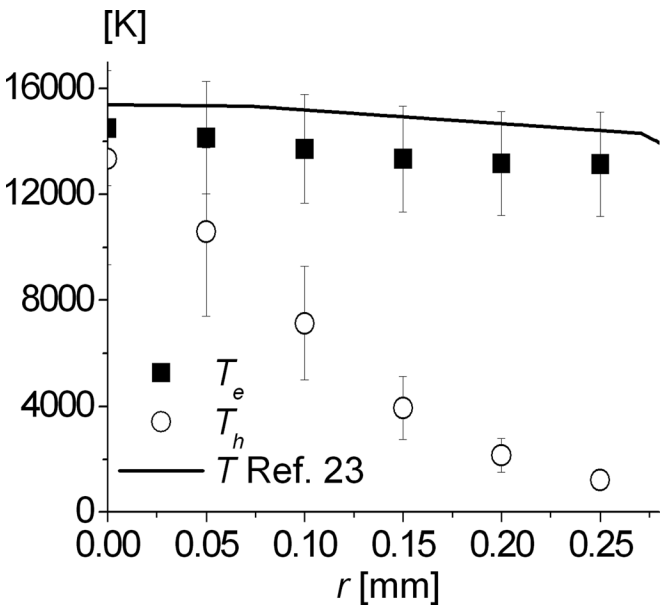

FIG. 6. Plasma temperature profiles obtained for the density profiles presented in Fig. 5 by using a generalized two-temperature Saha equation for 0.1 MPa. The LTE temperature profile previously obtained by the authors (Ref. 23) is also shown. Reprinted with permission from L. Prevosto, G. Artana, B. Mancinelli, and H. Kelly, J. Appl. Phys. **107**, 023304 (2010). Copyright © 2010 American Institute of Physics.

(1) An extensive region of the arc core is far from LTE. The LTE assumption appears valid only close to the arc center. This result is in accordance with Griem's criterion since an electron density exceeding 1.5×10^{23} m^{-3} was found at the arc axis.
(2) Substantial deviations from chemical equilibrium were found toward the arc core edge. Marked differences were obtained between the measured gas density values and those found in earlier work[23] for LTE. On the other hand, no significant deviations were found between the corresponding electron densities.
(3) Large deviations from kinetic equilibrium were found at elevated electron temperatures toward the arc core edge. We inferred an electron temperature profile nearly constant through the arc core, with a value of about 14 000–15 000 K, well decoupled from the heavy particle temperature (that reaches about 1500 K at the arc edge). Within the experimental uncertainty, no differences between the electron and LTE temperature were found.

ACKNOWLEDGMENTS

This work was supported by grants from the Universidad de Buenos Aires (PID X108), CONICET (PIP 5378), and Universidad Tecnológica Nacional (PID Z 012). G.A. and H.K. are members of CONICET.

[1]V. A. Nemchinsky and W. S. Severance, J. Phys. D: Appl. Phys. **39**, R423 (2006).
[2]M. Boulos, P. Fauchais, and E. Pfender, *Thermal Plasmas, Fundamentals and Applications* (Plenum, New York, 1994), Vol 1.
[3]P. Fauchais and A. Vardelle, IEEE Trans. Plasma Sci. **25**, 1258 (1997).
[4]K. Hsu and E. Pfender, J. Appl. Phys. **54**, 4359 (1983).
[5]J. Haidar, J. Phys. D: Appl. Phys. **28**, 2494 (1995).
[6]J. Haidar, J. Phys. D: Appl. Phys. **32**, 263 (1999).
[7]J. Jenista, J. V. R. Heberlein, and E. Pfender, IEEE Trans. Plasma Sci. **25**, 883 (1997).
[8]S. C. Snyder, G. D. Lassahn, and L. D. Reynolds, Phys. Rev. E **48**, 4124 (1993).
[9]R. E. Bentley, J. Phys. D: Appl. Phys. **30**, 2880 (1997).
[10]J. González-Aguilar, C. Pardo Sanjurjo, A. Rodríguez-Yunta, and M. A. G. Calderón, IEEE Trans. Plasma Sci. **27**, 264 (1999).
[11]P. Freton, J. J. Gonzalez, A. Gleizes, F. Camy-Peyret, G. Caillibotte, and M. Delzenne, J. Phys. D: Appl. Phys. **35**, 115 (2002).
[12]P. Freton, J. J. Gonzalez, F. Camy-Peyret, and A. Gleizes, J. Phys. D: Appl. Phys. **36**, 1269 (2003).
[13]V. Colombo, A. Concetti, E. Ghedini, S. Dallavalle, and M. Vancini, IEEE Trans. Plasma Sci. **36**, 389 (2008).
[14]Q. Zhou, H. Li, X. Xu, F. Liu, S. Guo, X. Chang, W. Guo, and P. Xu, J. Phys. D: Appl. Phys. **42**, 015210 (2009).
[15]S. Ghorui, J. V. R. Heberlein, and E. Pfender, J. Phys. D: Appl. Phys. **40**, 1966 (2007).
[16]L. Prevosto, H. Kelly, and B. Mancinelli, J. Appl. Phys. **105**, 013309 (2009).
[17]L. Prevosto, H. Kelly and B. Mancinelli, J. Appl. Phys. **105**, 123303 (2009).
[18]L. Schott, in *Plasma Diagnostics*, edited by W. Lochte-Holtgreven (AIP, New York, 1995), Chapter 3, pp. 668–725.
[19]C. Pardo J. González-Aguilar, A. Rodríguez-Yunta, and M. A. G. Calderón, J. Phys. D: Appl. Phys. **32**, 2181 (1999).
[20]L. Girard, Ph Teulet, M. Razafinimanana, A. Gleizes, F. Camy-Peyret, E. Baillot, and F. Richard, J. Phys. D: Appl. Phys. **39**, 1543 (2006).
[21]J. Peters, J. Heberlein, and J. Lindsay, J. Phys. D: Appl. Phys. **40**, 3960 (2007).
[22]G. S. Settles, *Schlieren and Shadowgraph Techniques*, (Springer, Berlin, 2001).
[23]L. Prevosto, G. Artana, B. Mancinelli, and H. Kelly, J. Appl. Phys. **107**, 023304 (2010).
[24]M. C. M. van de Sanden, P. P. J. M. Schram, A. G. Peeters, J. A. M. van der Mullen, and G. M. W. Kroesen, Phys. Rev. A **40**, 5273 (1989).
[25]L. Prevosto, H. Kelly, and B. Mancinelli, IEEE Trans. Plasma Sci. **37**, 1092 (2009).
[26]S. Ghorui, J. V. R. Heberlein, and E. Pfender, Plasma Chem. Plasma Process. **27**, 267 (2007).
[27]L. Prevosto, H. Kelly, and B. Mancinelli, J. Appl. Phys. **106**, 053308 (2009).